Published in final edited form as:
Cancer Res. 2013 October 15; 73(20): 6346–6358. doi:10.1158/0008-5472.CAN-13-1385.

Activation of MAPK pathways due to DUSP4 loss promotes cancer stem cell-like phenotypes in basal-like breast cancer

Justin M. Balko[1,3], **Luis J. Schwarz**[1,4], **Neil E. Bhola**[1], **Richard Kurupi**[1], **Phillip Owens**[2], **Todd W. Miller**[5], **Henry Gómez**[4], **Rebecca S. Cook**[2,3], and **Carlos L. Arteaga**[1,2,3]

[1]Department of Medicine, Vanderbilt-Ingram Cancer Center, Vanderbilt University, Nashville, TN

[2]Department of Cancer Biology, Vanderbilt-Ingram Cancer Center, Vanderbilt University, Nashville, TN

[3]Department of Breast Cancer Research Program, Vanderbilt-Ingram Cancer Center, Vanderbilt University, Nashville, TN

[4]Instituto Nacional de Enfermedades Neoplásicas, Lima, Perú

[5]Department of Pharmacology & Toxicology, Norris Cotton Cancer Center, Geisel School of Medicine at Dartmouth, Lebanon, NH

Abstract

Basal-like breast cancer (BLBC) is an aggressive disease that lacks a clinically-approved targeting therapy. Traditional chemotherapy is effective in BLBC, but it spares the cancer stem cell (CSC)-like population which is likely to contribute to cancer recurrence after the initial treatment. DUSP4 is a negative regulator of the MAPK pathway that is deficient in highly aggressive BLBCs treated with chemotherapy, leading to aberrant MAPK activation and resistance to taxane-induced apoptosis. Herein, we investigated how DUSP4 regulates the MEK and JNK pathways in modifying CSC-like behavior. DUSP4 loss increased mammosphere formation and the expression of the CSC-promoting cytokines IL-6 and IL-8. These effects were caused in part by loss of control of the MEK and JNK pathways and involved downstream activation of the ETS-1 and c-JUN transcription factors. Enforced expression of DUSP4 in reduced the CD44+/CD24- population in multiple BLBC cell lines in a MEK-dependent manner, limiting tumor formation of claudin-low SUM159PT cells in mice. Our findings support the evaluation of MEK and JNK pathway inhibitors as therapeutic agents in BLBC in order to eliminate the CSC population.

Keywords

Breast cancer; DUSP4; MEK; JNK; cancer stem cell

Corresponding author: Carlos L. Arteaga, Vanderbilt University Medical Center, 2200 Pierce Ave, 777 PRB, Nashville, TN 37232-6307, carlos.arteaga@vanderbilt.edu, Phone: (615) 936-3524, Fax: (615) 936-1790.

Conflicts of interest: N/A

Introduction

Despite the advent of molecularly targeted therapies in the treatment of breast cancer, conventional chemotherapy remains the main treatment for basal-like breast cancer (BLBC). BLBC is a molecular subtype characterized by gene expression patterns and immunohistochemical markers of the basal myoepithelium (1). It is comprised primarily of 'triple-negative' tumors which lack detectable estrogen receptor-α (ER), progesterone receptor (PR) and amplification of the HER-2/ERBB2 receptor (1).

BLBC cell lines can be further segregated into two subgroups based on transcriptomic and phenotypic differences: Basal A and Basal B (2-4). Basal B cancer cell lines represent those highly invasive cells, which demonstrate epithelial-to-mesenchymal (EMT) and cancer stem-cell (CSC)-like phenotypes (2, 4). Basal B expression patterns and phenotypes have been identified in human and mouse mammary tumors of the 'claudin-low' subtype (5, 6) and are highly enriched for $CD44^+/CD24^-$ cells (2), which mark the EMT cell population that also contains CSC-like traits. Importantly, many BLBC tumors and cell lines enriched for these characteristics are resistant to conventional chemotherapy (7). Further, drug-resistant cancer cell subpopulations are selected by treatment with chemotherapy, enriching for cells with a more aggressive phenotype (5, 7). In contrast, Basal A tumors lack EMT and CSC markers and express both CD44 and CD24 (2).

Because of the relative poor outcome of patients with BLBC, defining the molecular pathways altered in this cancer subtype remains at the forefront of translational research. It has been established that Ras/MEK/ERK activity can induce EMT (8), a trait of the tumor-initiating or CSC-like population and the claudin-low subtype (8-12). Given that *Ras* and *Raf* mutations are rare in breast cancer (13, 14), we hypothesized that alternative mechanisms of MAPK activation may play a role in promoting CSC-like traits. We propose that loss of *Dual Specificity Phosphatase-4* (*DUSP4*), a phosphatase against ERK1/2 and JNK1/2 (15), is one of those mechanisms. Indeed, we recently identified DUSP4 deficiency as a mediator of docetaxel resistance in triple negative breast cancer, basal-like gene expression and high MEK activity (16).

Herein, we show that genomic *DUSP4* loss is a frequent event in many cancer types, but is more pronounced in aggressive breast cancer subtypes. In BLBC cell lines, DUSP4 modulated the expression of $CD44^+/CD24^-$ markers, mammosphere formation and tumor initiation. DUSP4 also regulated expression and phosphorylation of cJUN and ETS-1 transcription factors and expression of IL-6 and IL-8. Restoration of DUSP4 expression in BT549 and SUM159PT BLBC cell lines reduced the $CD44^+/CD24^-$ compartment. CSC-enriched SUM159PT cells with temporally controlled DUSP4 expression demonstrated reduced tumorigenicity. Cells where DUSP4 expression was enforced eventually lost the DUSP4 transgene and restored the $CD44^+/CD24^-$ population, suggesting that DUSP4 elicits tumor suppressor function. Collectively, these results suggest that DUSP4 is a tumor suppressor which is lost in breast cancer and can influence CSC traits. We propose that in patients with DUSP4 deficient breast cancer, therapeutic inhibition of MEK and JNK may complement chemotherapy in targeting CSCs.

Methods

Cell culture

ZR75-1, MDA-231, MDA-468 and 293FT cells were maintained in DMEM (GIBCO) supplemented with 10% fetal bovine serum (FBS; GIBCO). BT-549 and HCC1143 cells were maintained in RPMI (GIBCO) supplemented with 10% FBS. SUM159PT cells were maintained in DMEM supplemented with 5% FBS and 0.5 μg/mL hydrocortisone. MFM223 luminal AR(22) cells were maintained in MEM + 10% FBS, supplemented with Insulin/ Transferrin/Selenium (GIBCO).

Xenograft studies

MDA-231 xenografts were generated and treated as previously described (16). For the temporally controlled DUSP4 pINDUCER model, athymic nu/nu mice (Harlan Sprague Dawley) were primed with DOX (2 mg/mL in 5% sucrose, ad libitum) or 5% sucrose (control) for 2 days prior to injection. SUM159PT/pINDUCER-DUSP4 or parental SUM159PT cells were primed for 4 days with 2 ng/mL DOX prior to injection. Ten thousand cells were injected in Matrigel (BD Biosciences) into the left (pINDUCER cells) or right (parental cells) mammary fatpad. DOX was continually administered in drinking water for a period of 60 days prior to sacrifice and examination for tumor formation.

Adenovirus transduction

Transduction and validation of GFP-expressing (AdGFP) adenovirus was conducted as previously reported (46). Adenovirus expressing DUSP4 (AdDUSP4) was purchased from Vector Biolabs (Philadelphia, PA).

Reagents and chemicals

Recombinant human IL-6 and IL-8 were purchased from R&D Systems, reconstituted in phosphate buffered saline and utilized at a final concentration of 10 ng/mL and 100 ng/mL, respectively. Selumetinib, U0126, SP600125 and CI1040 were purchased from Selleck Chem, dissolved in DMSO, and utilized at a final concentration of 1 μM, 10 μM, 10 μM and 1μM, respectively. Hydrocortisone and B27 supplement were purchased from Sigma.

Immunoblotting, ELISA, and cytokine arrays

Immunoblotting was carried out as described (46). Antibodies used for immunoblotting were: p-ERK1/2 (p-T202/Y204; #9101), calnexin (#2433), p-cJUN (#2361), cJUN (#9165), p-JNK1/2 (#4668), JNK1/2 (#9252) (all from Cell Signaling), p-ETS-1(p-T38, Invitrogen 44-1104G), ETS-1 (Santa Cruz sc-350), DUSP4 (Cell Signaling #5419), Anti-HA tag (Santa Cruz sc-805) and actin (Sigma, A2066). ELISAs (IL-6 and IL-8 Quantikine; R&D Systems) and cytokine arrays (RayBioTech) were performed according to the manufacturer's protocol.

siRNA transfection

Cells were reverse-transfected in 6-well dishes or 60-mm dishes with 20 nM siRNA using Dharmafect 1 (MDA-231, BT549) or Dharmafect 4 (SUM159PT) reagents according to the manufacturer's protocol. siRNAs targeting *DUSP4* (sequence #9: Thermoscientific cat#

J-003963-09; sequence #72: Invitrogen cat# s4372; sequence #73: Invitrogen cat# s4373), *ETS1* (Thermoscientific cat# M-003887-00-0005), or *CJUN* (Thermoscientific cat# M-003268-03-0005), or non-silencing control (Thermoscientific cat# D-001810-10). For mammosphere assays, cells were trypsinized and counted after 24 hrs and then replated to ultra-low attachment, 6-well or 24-well plates (Corning).

Flow cytometry

Cells were passed through a 35-μm filter, pelleted, washed in 1X phosphate buffered saline (PBS) + 1% FBS, and counted. One million cells were suspended in 1X PBS + 1% FBS and stained with anti-CD44-APC conjugate and anti-CD24-PE conjugate (BD Biosciences) for 30 min at 4°C. Cells were washed 3 times and then analyzed by flow cytometry.

Quantitative real-time PCR

RNA was isolated with RNEasy kits (Qiagen) and 1 μg total RNA was used to synthesize cDNA using the iScript kit (BioRad). qRT-PCR was performed on a Biorad IQ thermacycler. Standard curves were generated to estimate efficiency and the ΔΔCT method was used to quantitate fold change. Primer details are available in Supplementary Methods.

Chromatin immunoprecipitation

Chromatin immunoprecipitation (ChIP) was performed as previously described (47). MDA-231 cells were treated for 16 hr with selumetinib (1 μM) prior to harvest; cell lysates were prepared and immunoprecipitated with an ETS-1 antibody (Santa Cruz sc-350) or rabbit IgG control. The promoter regions -10,000 to +2000 for IL6 and IL8 were evaluated using ChipMapper (48). Two regions containing ETS sites were selected. Primer details are available in Supplementary Methods.

Molecular cloning

The *DUSP4* open reading frame without a stop codon was obtained from Open Biosystems (Accession EU831550) and was recombined into the pINDUCER-22 plasmid(36) using LR Clonase (Invitrogen), resulting in DOX-inducible *DUSP4-HA* transgene expression. Short-hairpins targeting *DUSP4* or non-targeting control (Cat#RHS4348) in pGIPZ were purchased from Open Biosystems (clone IDs: V3LHS_333999, V3LHS_334001, V3LHS_334002, V2LHS_118839) and cloned into pINDUCER-11(36) using XhoI and MluI sites and screened for efficacy in 293FT cells. Lentiviral particles were produced by co-transfecting pINDUCER-DUSP4 (short-hairpin or ORF) plasmid with pMD2G and psPAX helper plasmids into 293FT cells. Target cells were transduced in the presence of polybrene and selected for GFP expression by FACS. The LacZ gene was also cloned into pINDUCER22 vector as a transgene control in selected experiments.

Mammosphere assays

Mammosphere assays were performed by plating 10^4 cells in serum free DMEM/F12 1:1 media (Gibco) supplemented with EGF (20 ng/mL) and B27 (2%). MDA-231 mammospheres were grown in the absence of B27. Mammospheres were allowed to form for 3-7 days and were scanned and visualized by GelCount (Oxford Optronics; Oxford, UK).

Mammospheres greater than 100 μm in diameter were counted and average volume was estimated using the software's (size × density) function. Total mammosphere volume/well was calculated as volume × sphere number.

Microarrays

MDA-231, BT549, and SUM159PT cells were harvested 96 hr after siRNA transfection with siDUSP4 or siCONTROL. siCONTROL cells were also treated with selumetinib (1 μM) 4 or 24 hr prior to harvest. RNA was isolated with RNEasy kits according to the manufacturer's protocol. Microarrays were performed by the Vanderbilt Genome Sciences Resource. Additional details regarding analysis, including the acquisition and analysis of publically available datasets are available in Supplementary Methods.

Statistical analysis

Statistical analyses (linear regression, ANOVA and student's t-tests) were performed in R (http://cran.r-project.org) and Graphpad Prism (GraphPad Software, La Jolla, CA). For two-group analyses, t-tests were performed. In >2 group analyses, ANOVA was performed with Tukey's post-hoc analyses to compare individual groups.

Results

MEK pathway activity coupled with repression of DUSP4 feedback correlates with CSC features

We have reported that methylation of the *DUSP4* gene is a frequent event in BLBC. However, the frequency of *DUSP4* copy loss, as part of the 8p11-21 region of frequent copy number alterations (17-19), has not been well established. We utilized the Cancer Cell Line Encyclopedia (CCLE), which integrates genomic data on over 600 cancer cell lines to determine if *DUSP4* copy loss is a frequent event in breast and other types of cancer cells. *DUSP4* copy loss was common across all cancer cell lines, with breast cancer cells demonstrating the lowest median copy number ratio (Fig. 1A). Next, we examined *DUSP4* copy number changes in 444 breast cancers and normal breast specimens from The Cancer Genome Atlas (TCGA). Apparent peaks in the frequency distribution histograms demonstrated common hemi- and homozygous deletion events at this locus, which were most frequent in basal-like, HER2-enriched and luminal B cancers (Fig. 1B), while copy number gains were rare. These molecular subtypes represent the most aggressive and/or chemotherapy-resistant breast cancers. Importantly, DUSP4 copy number ratio across the samples correlated strongly to DUSP4 gene expression (Supplementary Fig. S1).

DUSP4 has phosphatase activity against JNK1/2 and ERK1/2, suggesting that activation of these pathways upon DUSP4 loss drives phenotypes associated with aggressive forms of breast cancer. We utilized a gene expression signature of MEK activity (16, 20) to determine whether transcriptional output of MEK identifies BLBC cell lines with CSC-like traits, using a ratio of *CD44:CD24* mRNA expression as a read out. Expression of *CD44* and *CD24* is a differentiating factor of luminal, Basal A (basal-like, epithelial characteristics), and Basal B (EMT and CSC enriched) cell lines (2). The MEK signature score was strongly associated

with the *CD44:CD24* mRNA ratio (P=0.00064) in the ICBP50 panel of breast cancer cell lines (Fig. 1C).

Next, we determined whether the MEK signature score was associated with the CSC trait of mammosphere formation (7, 20). The MEK signature score was high in mammospheres derived from primary breast tumors but not in RNA extracted from the matched primary tumors (Fig. 1D-E; P<0.0001) (7), suggesting that MEK activation is upregulated in the CSC-like population. Furthermore, *DUSP4* mRNA expression was negatively associated with the CD44:CD24 mRNA ratio in the ICBP50 panel, specifically in cell lines with a high MEK score (Fig. 1F). This distinction is important, as *DUSP4* is an immediate early gene that is upregulated following MEK activation under normal conditions (21). Thus, in cell lines with low MEK activity, *DUSP4* expression would also be expected to be low. However, in a MEK-activated cell line, *DUSP4* downregulation (via copy loss or methylation) would result in unrestricted pathway activity.

Next, we profiled MEK and JNK pathway activation across a panel of breast cancer cell lines. The majority of BLBC cell lines demonstrated high expression and activation of the ETS-1 and cJUN transcription factors, which lie downstream of the DUSP4 targets, JNK1/2 and ERK1/2. These transcription factors were most highly expressed in the Basal B or claudin-low cell lines (MDA-231, SUM159PT and BT549), which also exhibit CSC-like properties (2, 4, 5). Baseline DUSP4 expression was lower in Basal B cell lines compared Basal A and luminal cell lines, including the luminal/androgen receptor expressing MFM223 (22), with the exception of MDA-231 cells. MDA-231 cells, which harbor mutant $KRAS^{G13D}$, had higher DUSP4 expression than the other cell lines tested, consistent with findings in colorectal cancer where KRAS mutations have been shown to upregulate *DUSP4* expression to compensate for enhanced MEK pathway activity (23). Since this cell line has basal-like expression associated with considerable *DUSP4* expression and, as such, represents an ideal model to study loss of *DUSP4* function.

Loss of DUSP4 enhances mammosphere formation and MEK- and JNK-dependent IL6 and IL8 expression

In MDA-231 cells, downregulation of DUSP4 by each of three siRNAs resulted in an increase in JNK activity as measured by cJUN phosphorylation and mammosphere volume relative to control siRNA (Fig. 2A-B). siRNA construct #73 produced a more subtle phenotype than the other constructs, despite apparent efficient DUSP4 knockdown. Longer exposures revealed residual DUSP4 expression with this siRNA, which was confirmed by qRT-PCR (data not shown), providing a possible explanation to the variability between effect sizes observed with the siRNAs. An increase in ERK activation could not be observed, possibly due to the high intrinsic activation level of this pathway in MDA-231 cells. However, both cJUN and ETS-1, downstream targets of JNK and ERK respectively, showed increased levels and/or activation upon loss of DUSP4 in non-adherent conditions (Fig. 2C). To determine if this phenotype was cell-autonomous, we cultured SUM159PT cells as mammospheres in serum-free media conditioned by MDA231 cells treated with siCONTROL or siDUSP4. Conditioned medium from MDA-231/siDUSP4 cells stimulated SUM159PT mammosphere formation 2-3 fold compared to medium from MDA-231/

siCONTROL cells, suggesting that loss of DUSP4 resulted in the secretion of mammosphere-stimulating paracrine factors (Fig. 2D). Cytokine arrays of conditioned media showed that interleukin-6 (IL6), a cytokine that stimulates CSC expansion (24-27), was upregulated following *DUSP4* knockdown (Supplementary Fig. S2), and this effect was primarily transcriptional (Fig. 2E-F). IL-8 was also moderately increased in the conditioned media. *DUSP4* knockdown using a doxycycline-inducible DUSP4 shRNA (shDUSP4) resulted in upregulation of both *IL6* and *IL8* when the cells were cultured for longer time periods (>10 days; Supplementary Fig. S3). However, transcriptional upregulation of IL8 was not observed following transient DUSP4 knockdown using siRNA (data not shown). Transcriptional upregulation of *IL6* was partially blocked by MEK (selumetinib/AZD6244) inhibition, but not by the JNK inhibitor (SP600125), while the combination had the most profound effect (Fig. 2G). cJUN phosphorylation and expression were downregulated by both the MEK and JNK inhibitors, with maximal inhibition by the combination (Fig. 2H). This is consistent with previous reports that both ERK and JNK can regulate cJUN (28-30). Combined inhibition of both MEK and JNK abrogated the upregulation of MDA-231 mammosphere growth observed upon knockdown of DUSP4 with siRNA (Fig. 2I).

To determine the specificity of the MEK pathway in tumor self-renewal in MDA-231 cells, we performed the mammosphere assay in the presence of two additional MEK inhibitors (U0126 and CI-1040), or the dual PI3K/mTOR inhibitor BEZ235 (31). Under basal conditions, only U0126 reduced primary mammosphere growth. However, after the spheres were collected trypsinized, and re-plated in the absence of drug, no spheres formed in plates treated with either MEK inhibitor. Spheres treated with DMSO control reformed quickly while BEZ235-treated spheres formed, albeit at a reduced rate. When the secondary spheres and residual cells were collected and plated under adherent conditions in the presence of serum, only the control and BEZ235-treated cells attached and resumed normal proliferation (Supplementary Fig. S4). *DUSP4 regulates IL6 and IL8 expression via ETS-1 and cJUN.* In two large breast cancer datasets, DUSP4 mRNA expression negatively correlated with *IL6* and *IL8* expression, suggesting that DUSP4 regulates the expression of these cytokines *in vivo* (Fig 3A). Furthermore, in the TCGA breast cancer dataset, genomic deletion of *DUSP4* was associated with high expression of cJUN phosphorylated at Ser73, a known activation site (Supplementary Fig. S5) (32). To determine if the JNK and MEK pathways regulate *IL6* and *IL8* expression in BLBC cells with low DUSP4 expression, we treated BT549 and SUM159PT cells with the MEK or JNK inhibitor or the combination. *IL8* and *IL6* mRNA expression and respective ligand secretion were inhibited to the greatest degree in both cell lines following treatment with the MEK inhibitor (Fig 3B-C), while the effect of the JNK inhibitor was more variable. Of note, in BT549, only the JNK inhibitor downregulated *IL6* transcription, but this downregulation did not translate into reduced IL-6 ligand in the conditioned media. Only the MEK inhibitor downregulated total ETS-1 or T38 P-ETS-1 levels (T38; is phosphorylated by ERK1/2), while the MEK and JNK inhibitors additively reduced total cJUN and P-cJUN levels (Fig. 3D). These results support the previously reported crosstalk between the AP-1 (cJUN and cFOS) and ETS-1 transcription factors (33, 34). Finally, in MDA-231 cells, chromatin immunoprecipitation (ChIP) with an ETS-1 antibody identified a binding region of ETS-1 in the *IL8* promoter, and ETS-1 was abrogated by treatment with the MEK inhibitor selumetinib (Supplementary Fig. S6).

Adenoviral transduction of DUSP4 (AdDUSP4) recapitulated the effects of the JNK and MEK inhibitors by downregulating p-cJUN, cJUN, p-ETS-1, ETS-1, and p-JNK (Fig. 3E). Interestingly, DUSP4 overexpression did not decrease ERK1/2 phosphorylation. In BT549 and SUM159PT cells, DUSP4 overexpression significantly downregulated *IL6* and *IL8* transcription. siRNA knockdown of ETS-1 or cJUN in SUM159PT cells downregulated *IL6* and *IL8* transcription, suggesting that these transcription factors contribute to expression of this CSC-promoting cytokine (Fig. 3G-H).

MEK regulates mammosphere growth in an IL-6- and/or IL-8-dependent manner in BLBC

Next, we tested whether MEK inhibition would reduce mammosphere growth. Selumetinib treatment inhibited SUM159PT and BT549 mammosphere growth (Fig. 4A-B). Reconstitution with recombinant IL-6 (BT549) or the combination of IL-6 and IL-8 (SUM159PT) restored this phenotype (Fig. 4B). Similar effects were observed with the MEK inhibitors U0126 and CI1040 in SUM159PT cells (Supplementary Fig. S7A). Furthermore, when viable mammospheres were dissociated and re-plated in the absence of drug, a significant impact on secondary mammosphere formation was also observed (Supplementary Fig. S7B).

Taxanes have been shown to spare CSCs (7, 35). To determine whether this is due to drug-induced expression of CSC-promoting cytokines, we utilized MDA-231 xenografts treated for 4 weeks with docetaxel, selumetinib or the combination of both drugs (16). Xenografts from docetaxel-treated mice exhibited markedly higher levels *IL6* and *IL8* mRNA levels compared to control-treated tumors (Fig. 4C). Co-treatment with selumetinib partially inhibited this upregulation, suggesting MEK inhibitors may be an effective therapeutic complement to taxanes in BLBC. When tumors were dissociated and plated in a mammosphere assay, cells from selumetinib-treated tumors formed smaller and fewer mammospheres, while tumor cells derived from tumors treated with the combination did not form spheres (Fig. 4D). Further, cells dissociated from xenografts that had been treated with the combination of selumetinib and docetaxel contained fewer $CD44^{+}/CD24^{-}$ cells compared to the other treatment groups as analyzed by FACS (Fig. 4E).

Gene expression changes following DUSP4 loss resemble BLBC

Next, we examined global gene expression changes induced by siRNA-mediated DUSP4 loss or treatment with selumetinib for 4 or 24 hr in MDA-231, SUM159PT and BT549 cells. The genes modulated by DUSP4 siRNA in MDA-231 cells (which have higher expression of DUSP4) tended to oppose those modulated by the MEK inhibitor (Fig 5A). For example, when comparing siDUSP4 transfection to 24 hr treatment with selumetinib, 24% of genes demonstrated directional concordance consistent with the known biology of DUSP4 (i.e., were upregulated by DUSP4 knockdown and downregulated by the MEK inhibitor). However, 19% of genes demonstrated discordance (i.e., were upregulated by both *DUSP4* knockdown and selumetinib). MDA-231 cells demonstrated the most profound gene expression changes following siDUSP4 transfection. We took the significantly changed genes (up and down regulated) identified in MDA-231 cells and scored the other cell lines using this signature. siDUSP4 treatment induced similar changes in SUM159PT and BT549 cells, albeit it to a lesser extent than in MDA-231 cells (Fig 5B). Interestingly, treatment

with selumetinib for 4 or 24 hr only moderately decreased the DUSP4-loss score, suggesting that loss of *DUSP4* also modulates MEK-independent gene expression. These effects of *DUSP4* loss may also reflect derepression of the JNK pathway, or other yet undiscovered function(s) of DUSP4.

Consistent with our report that *DUSP4* loss reduces the chemosensitivity of MDA-231 cells (16), a number of genes associated with drug resistance (another CSC/tumor initiating trait) were also upregulated following *DUSP4* knockdown, including *ERCC6*, *RRM2* and *ABCG2* (Fig. 5C). To test how the signature of *DUSP4* loss correlates with the molecular subtypes of breast cancer, we plotted the TCGA breast cancer gene expression data (N=444) and the siDUSP4 score; gene expression patterns induced by loss of *DUSP4* most closely resembled those of BLBC (Fig. 5D). Further, *DUSP4* loss in MDA231 cells significantly altered genes associated with the claudin-low subtype, a CSC enriched-phenotype (5). In these cells, the claudin-low score was reduced by selumetinib treatment (Fig. 5E). These data suggest that DUSP4 loss transcriptionally activates programs associated with basal-like and claudin-low breast cancer.

Enforced DUSP4 expression regulates CD44/CD24 and tumor initiation

To determine whether enforced expression of DUSP4 alters the $CD44^+/CD24^-$ population in BLBC, we utilized the pINDUCER rtTA system (36) to conditionally express DUSP4 in SUM159PT and BT549 cells. We detected HA-tagged DUSP4 expression within 24 hrs of DOX treatment (2 ng/mL, data not shown). Cells were cultured in DOX for 0-10 days and analyzed by flow cytometry for CD44 and CD24 expression. Both BT549 and SUM159PT are claudin low/Basal B cell lines (4, 5) with a high population of tumor-initiating $CD44^+/CD24^-$ cells. After DOX treatment, CD24 expression was markedly increased, shifting the population away from $CD44^+/CD24^-$; this effect was maximal at 4 days (Fig. 6A and Supplementary Fig. S8A). Similarly, cells treated for 4 days with selumetinib substantially upregulated the $CD24^+$ population. The JNK inhibitor had only a modest effect (Supplementary Fig. S8B). These findings are supported by the previous microarray data showing upregulation of *CD24* mRNA upon 24 hr of selumetinib. They also imply that MEK activation modulates CD24 expression. Importantly, high CD24 and high CD44 expression is a defining feature of the Basal A subtype (2), suggesting that MEK inhibition may ‘convert’ mesenchymal BLBCs to those with epithelial and thus less aggressive features. Recombinant IL-6 and/or IL-8 co-administered with DOX to SUM159PT/pINDUCER-DUSP4 cells did not restore the $CD44^+/CD24^-$ population, suggesting that enforced DUSP4 expression decreases IL6 and IL8 expression as well as alters the $CD44^+/CD24^-$ population in *trans* and not in *cis* (Supplementary Fig. S8C). Doxycycline treatment of SUM159PT/pINDUCER-DUSP4 cells also decreased mammosphere formation *in vitro* (Fig. 6B). To determine whether enforced DUSP4 expression is sufficient to reduce the tumor-initiating population *in vivo*, we pretreated SUM159PT/pINDUCER-DUSP4 cells with DOX for 2 days and injected 1×10^4 cells into the left mammary fatpad of athymic mice. Parental SUM159PT cells were utilized to control for the treatment effects of DOX and injected in the contralateral mammary fatpad. Following tumor cell inoculation, mice were treated +/- DOX for 60 days and monitored for tumor formation (Fig. 6C-D). At 60 days, tumors were apparent in 4/5 mice injected with SUM159PT/pINDUCER-DUSP4 cells

whereas no DOX-supplemented mice developed obvious tumors. On microscopic inspection of the injection site, one mouse treated with DOX showed viable SUM159PT/pINDUCER-DUSP4 cells, suggesting delayed tumor development. This could be partially explained by the observation that after 30 days of DUSP4 induction with DOX, SUM159PT cells downregulated the transgene and restored their original $CD44^+/CD24^-$ population (Supplementary Fig. S9). Collectively, these results suggest that 1) enforced DUSP4 expression reduces the tumor-initiating population in BLBC and 2) *DUSP4* has a tumor suppressor function in BLBC.

Discussion

Conventional chemotherapies spare CSC-like tumor cells, leading to the outgrowth of resistant subpopulations that repopulate the tumor (7). An increasing body of literature suggests that the CSC population exhibits plasticity, thus implying that cancer cells can shift between CSC and non-CSC phenotypes (37). Therefore, therapies that target the CSC population in a tumor would be an effective approach to treatment. Herein, we have explored the role of the DUSP4 phosphatase in regulating CSC-like traits in BLBC. We show that DUSP4 is lost in breast cancer at high frequency. Loss of function studies in MDA-231 cells demonstrated that DUSP4 suppresses ETS-1 and cJUN activity. Relief from DUSP4-mediated negative feedback upregulates IL-6 and IL-8 in a MEK and JNK dependent manner, while enforced DUSP4 expression downregulates IL-6 and IL-8 expression, decreases the $CD44^+/CD24^-$ CSC-like population and reduces tumorigenicity. These effects of DUSP4 are mainly regulated via the MEK pathway, although suppression of JNK signaling contributes as well, possibly via cross talk between ETS-1 and cJUN.

Our findings linking aberrant MEK activity and CSC-like traits are consistent with concepts proposed by prior studies. In particular, Morel and colleagues showed that immortalized primary breast epithelial cells were primarily $CD44^+/CD24^+$, while the same cells transformed with activated HRAS (G12V) became $CD44^+/CD24^-$ (8). These cells, originally generated and characterized by Weinberg and colleagues (38), underwent EMT and acquired stem cell properties following transduction with HRAS. This result parallels our finding that CD24 expression is acquired in BT549 and SUM159PT BLBC cells following enforced DUSP4 expression.

There are several limitations to these studies. While mammosphere formation and CD44/CD24 expression are not absolute CSC markers, the use of these assays enriches for CSC-like traits (39, 40). The majority of breast cancer cells grown as mammospheres are $CD44^+/CD24^-$, while only 10-20% of these possess tumor-initiating properties (41). Other attempts have been made to further enrich the CSC population using a variety of markers, including PROCR, EPCAM and functional aldehyde dehydrogenase activity (ALDEFLUOR assay) (24, 42-44). However, many of these markers are cell-line specific (44), which complicates analysis across multiple cell lines, and are not as well-established as CD44/CD24. Secondly, enforced DUSP4 expression had a more pronounced phenotype in the SUM159PT cell line compared to the BT549 cell line. DUSP4 expression simultaneously downregulated *IL6* and *IL8* expression in SUM159PT cells whereas only IL8 was markedly affected in the BT549 line. Likewise, SUM159PT cells escaped enforced DUSP4 expression after 30 days,

whereas BT549 cells did not, suggestive of an 'acquired' tolerance to DUSP4 expression in SUM159PT cells, whereas an intrinsic resistance was present in BT549 cells. Importantly, BT549 cells are PTEN-null resulting in deregulated high PI3K activity. This alteration may represent a mechanism for dispensability of MEK and JNK activity during enforced DUSP4 expression. Indeed, other investigators have shown that aberrant PI3K activity can also maintain the claudin-low phenotype (45).

In summary, DUSP4 is frequently lost in breast cancer, representing a mechanism of MEK and JNK activation which drives CSC-like traits, including mammosphere formation, *IL6* and *IL8* expression, CD44/CD24 expression patterns and tumor formation. Although these traits are not linearly connected, they appear to predominate from DUSP4-mediated control over the cJUN and ETS-1 transcription factors. Treatment of DUSP4-deficient BLBC with MEK and potentially JNK inhibitors may improve outcomes by affecting the CSC-like population of tumor cells and thus complement conventional anticancer chemotherapy in this subtype of breast cancer.

Supplementary Material

Refer to Web version on PubMed Central for supplementary material.

Acknowledgments

The authors would like to acknowledge the patients and researchers in The Cancer Genome Atlas (TCGA) Breast Cancer Group and Dr. Barbara Graves (University of Utah) for providing ETS-1 ChIP protocols.

Financial support: This work was supported by the NIH Breast Cancer Specialized Program of Research Excellence (SPORE) grant P50 CA98131, Vanderbilt-Ingram Cancer Center Support grant P30 CA68465, Vanderbilt Digestive Disease Center grant P30 DK58404, Vanderbilt Vision Center grant P30 EY08126, K99/R00 CA142899 (TWM), National Institutes of Health R01CA143126 (RSC) and Susan G. Komen for the Cure Foundation grants SAC100013 (CLA), KG100677 (RSC), and PDF12229712 (JMB).

References

1. Perou CM, Sorlie T, Eisen MB, van de Rijn M, Jeffrey SS, Rees CA, et al. Molecular portraits of human breast tumours. Nature. 2000; 406:747–52. [PubMed: 10963602]
2. Blick T, Hugo H, Widodo E, Waltham M, Pinto C, Mani SA, et al. Epithelial mesenchymal transition traits in human breast cancer cell lines parallel the CD44(hi/)CD24 (lo/-) stem cell phenotype in human breast cancer. J Mammary Gland Biol Neoplasia. 2010; 15:235–52. [PubMed: 20521089]
3. Mirzoeva OK, Das D, Heiser LM, Bhattacharya S, Siwak D, Gendelman R, et al. Basal subtype and MAPK/ERK kinase (MEK)-phosphoinositide 3-kinase feedback signaling determine susceptibility of breast cancer cells to MEK inhibition. Cancer Res. 2009; 69:565–72. [PubMed: 19147570]
4. Neve RM, Chin K, Fridlyand J, Yeh J, Baehner FL, Fevr T, et al. A collection of breast cancer cell lines for the study of functionally distinct cancer subtypes. Cancer Cell. 2006; 10:515–27. [PubMed: 17157791]
5. Prat A, Parker JS, Karginova O, Fan C, Livasy C, Herschkowitz JI, et al. Phenotypic and molecular characterization of the claudin-low intrinsic subtype of breast cancer. Breast Cancer Res. 2010; 12:R68. [PubMed: 20813035]
6. Herschkowitz JI, Simin K, Weigman VJ, Mikaelian I, Usary J, Hu Z, et al. Identification of conserved gene expression features between murine mammary carcinoma models and human breast tumors. Genome Biol. 2007; 8:R76. [PubMed: 17493263]

7. Creighton CJ, Li X, Landis M, Dixon JM, Neumeister VM, Sjolund A, et al. Residual breast cancers after conventional therapy display mesenchymal as well as tumor-initiating features. Proc Natl Acad Sci U S A. 2009; 106:13820–5. [PubMed: 19666588]
8. Morel AP, Lievre M, Thomas C, Hinkal G, Ansieau S, Puisieux A. Generation of breast cancer stem cells through epithelial-mesenchymal transition. PLoS One. 2008; 3:e2888. [PubMed: 18682804]
9. Mani SA, Guo W, Liao MJ, Eaton EN, Ayyanan A, Zhou AY, et al. The epithelial-mesenchymal transition generates cells with properties of stem cells. Cell. 2008; 133:704–15. [PubMed: 18485877]
10. Asiedu MK, Ingle JN, Behrens MD, Radisky DC, Knutson KL. TGFbeta/TNF(alpha)-mediated epithelial-mesenchymal transition generates breast cancer stem cells with a claudin-low phenotype. Cancer Res. 2011; 71:4707–19. [PubMed: 21555371]
11. Liu M, Casimiro MC, Wang C, Shirley LA, Jiao X, Katiyar S, et al. p21CIP1 attenuates Ras- and c-Myc-dependent breast tumor epithelial mesenchymal transition and cancer stem cell-like gene expression in vivo. Proc Natl Acad Sci U S A. 2009; 106:19035–9. [PubMed: 19858489]
12. Morel AP, Hinkal GW, Thomas C, Fauvet F, Courtois-Cox S, Wierinckx A, et al. EMT inducers catalyze malignant transformation of mammary epithelial cells and drive tumorigenesis towards claudin-low tumors in transgenic mice. PLoS Genet. 2012; 8:e1002723. [PubMed: 22654675]
13. Sanchez-Munoz A, Gallego E, de Luque V, Perez-Rivas LG, Vicioso L, Ribelles N, et al. Lack of evidence for KRAS oncogenic mutations in triple-negative breast cancer. BMC Cancer. 2010; 10:136. [PubMed: 20385028]
14. Comprehensive molecular portraits of human breast tumours. Nature. 2012; 490:61–70. [PubMed: 23000897]
15. Jeffrey KL, Camps M, Rommel C, Mackay CR. Targeting dual-specificity phosphatases: manipulating MAP kinase signalling and immune responses. Nat Rev Drug Discov. 2007; 6:391–403. [PubMed: 17473844]
16. Balko JM, Cook RS, Vaught DB, Kuba MG, Miller TW, Bhola NE, et al. Profiling of residual breast cancers after neoadjuvant chemotherapy identifies DUSP4 deficiency as a mechanism of drug resistance. Nat Med. 2012
17. Armes JE, Hammet F, de Silva M, Ciciulla J, Ramus SJ, Soo WK, et al. Candidate tumor-suppressor genes on chromosome arm 8p in early-onset and high-grade breast cancers. Oncogene. 2004; 23:5697–702. [PubMed: 15184884]
18. Venter DJ, Ramus SJ, Hammet FM, de Silva M, Hutchins AM, Petrovic V, et al. Complex CGH alterations on chromosome arm 8p at candidate tumor suppressor gene loci in breast cancer cell lines. Cancer Genet Cytogenet. 2005; 160:134–40. [PubMed: 15993269]
19. Anbazhagan R, Fujii H, Gabrielson E. Allelic loss of chromosomal arm 8p in breast cancer progression. Am J Pathol. 1998; 152:815–9. [PubMed: 9502423]
20. Pratilas CA, Taylor BS, Ye Q, Viale A, Sander C, Solit DB, et al. (V600E)BRAF is associated with disabled feedback inhibition of RAF-MEK signaling and elevated transcriptional output of the pathway. Proc Natl Acad Sci U S A. 2009; 106:4519–24. [PubMed: 19251651]
21. Camps M, Nichols A, Arkinstall S. Dual specificity phosphatases: a gene family for control of MAP kinase function. FASEB J. 2000; 14:6–16. [PubMed: 10627275]
22. Lehmann BD, Bauer JA, Chen X, Sanders ME, Chakravarthy AB, Shyr Y, et al. Identification of human triple-negative breast cancer subtypes and preclinical models for selection of targeted therapies. J Clin Invest. 2011; 121:2750–67. [PubMed: 21633166]
23. Gaedcke J, Grade M, Jung K, Camps J, Jo P, Emons G, et al. Mutated KRAS results in overexpression of DUSP4, a MAP-kinase phosphatase, and SMYD3, a histone methyltransferase, in rectal carcinomas. Genes Chromosomes Cancer. 2010; 49:1024–34. [PubMed: 20725992]
24. Charafe-Jauffret E, Ginestier C, Iovino F, Wicinski J, Cervera N, Finetti P, et al. Breast cancer cell lines contain functional cancer stem cells with metastatic capacity and a distinct molecular signature. Cancer Res. 2009; 69:1302–13. [PubMed: 19190339]
25. Ginestier C, Liu S, Diebel ME, Korkaya H, Luo M, Brown M, et al. CXCR1 blockade selectively targets human breast cancer stem cells in vitro and in xenografts. J Clin Invest. 120:485–97. [PubMed: 20051626]

26. Kim MY, Oskarsson T, Acharyya S, Nguyen DX, Zhang XH, Norton L, et al. Tumor self-seeding by circulating cancer cells. Cell. 2009; 139:1315–26. [PubMed: 20064377]
27. Sansone P, Storci G, Tavolari S, Guarnieri T, Giovannini C, Taffurelli M, et al. IL-6 triggers malignant features in mammospheres from human ductal breast carcinoma and normal mammary gland. J Clin Invest. 2007; 117:3988–4002. [PubMed: 18060036]
28. Smeal T, Binetruy B, Mercola DA, Birrer M, Karin M. Oncogenic and transcriptional cooperation with Ha-Ras requires phosphorylation of c-Jun on serines 63 and 73. Nature. 1991; 354:494–6. [PubMed: 1749429]
29. Binetruy B, Smeal T, Karin M. Ha-Ras augments c-Jun activity and stimulates phosphorylation of its activation domain. Nature. 1991; 351:122–7. [PubMed: 1903181]
30. Hibi M, Lin A, Smeal T, Minden A, Karin M. Identification of an oncoprotein- and UV-responsive protein kinase that binds and potentiates the c-Jun activation domain. Genes Dev. 1993; 7:2135–48. [PubMed: 8224842]
31. Brachmann SM, Hofmann I, Schnell C, Fritsch C, Wee S, Lane H, et al. Specific apoptosis induction by the dual PI3K/mTor inhibitor NVP-BEZ235 in HER2 amplified and PIK3CA mutant breast cancer cells. Proc Natl Acad Sci U S A. 2009; 106:22299–304. [PubMed: 20007781]
32. Cerami E, Gao J, Dogrusoz U, Gross BE, Sumer SO, Aksoy BA, et al. The cBio cancer genomics portal: an open platform for exploring multidimensional cancer genomics data. Cancer Discov. 2012; 2:401–4. [PubMed: 22588877]
33. Oh YT, Yue P, Zhou W, Balko JM, Black EP, Owonikoko TK, et al. Oncogenic Ras and B-Raf proteins positively regulate death receptor 5 expression through co-activation of ERK and JNK signaling. J Biol Chem. 2012; 287:257–67. [PubMed: 22065586]
34. Spangler B, Kappelmann M, Schittek B, Meierjohann S, Vardimon L, Bosserhoff AK, et al. ETS-1/RhoC signaling regulates the transcription factor c-Jun in melanoma. Int J Cancer. 2012; 130:2801–11. [PubMed: 21732343]
35. Gupta PB, Onder TT, Jiang G, Tao K, Kuperwasser C, Weinberg RA, et al. Identification of selective inhibitors of cancer stem cells by high-throughput screening. Cell. 2009; 138:645–59. [PubMed: 19682730]
36. Meerbrey KL, Hu G, Kessler JD, Roarty K, Li MZ, Fang JE, et al. The pINDUCER lentiviral toolkit for inducible RNA interference in vitro and in vivo. Proc Natl Acad Sci U S A. 2011; 108:3665–70. [PubMed: 21307310]
37. Gupta PB, Fillmore CM, Jiang G, Shapira SD, Tao K, Kuperwasser C, et al. Stochastic state transitions give rise to phenotypic equilibrium in populations of cancer cells. Cell. 2011; 146:633–44. [PubMed: 21854987]
38. Elenbaas B, Spirio L, Koerner F, Fleming MD, Zimonjic DB, Donaher JL, et al. Human breast cancer cells generated by oncogenic transformation of primary mammary epithelial cells. Genes Dev. 2001; 15:50–65. [PubMed: 11156605]
39. Dontu G, Abdallah WM, Foley JM, Jackson KW, Clarke MF, Kawamura MJ, et al. In vitro propagation and transcriptional profiling of human mammary stem/progenitor cells. Genes Dev. 2003; 17:1253–70. [PubMed: 12756227]
40. Al-Hajj M, Wicha MS, Benito-Hernandez A, Morrison SJ, Clarke MF. Prospective identification of tumorigenic breast cancer cells. Proc Natl Acad Sci U S A. 2003; 100:3983–8. [PubMed: 12629218]
41. Ponti D, Costa A, Zaffaroni N, Pratesi G, Petrangolini G, Coradini D, et al. Isolation and in vitro propagation of tumorigenic breast cancer cells with stem/progenitor cell properties. Cancer Res. 2005; 65:5506–11. [PubMed: 15994920]
42. Charafe-Jauffret E, Ginestier C, Iovino F, Tarpin C, Diebel M, Esterni B, et al. Aldehyde dehydrogenase 1-positive cancer stem cells mediate metastasis and poor clinical outcome in inflammatory breast cancer. Clin Cancer Res. 16:45–55. [PubMed: 20028757]
43. Huang EH, Hynes MJ, Zhang T, Ginestier C, Dontu G, Appelman H, et al. Aldehyde dehydrogenase 1 is a marker for normal and malignant human colonic stem cells (SC) and tracks SC overpopulation during colon tumorigenesis. Cancer Res. 2009; 69:3382–9. [PubMed: 19336570]

44. Hwang-Verslues WW, Kuo WH, Chang PH, Pan CC, Wang HH, Tsai ST, et al. Multiple lineages of human breast cancer stem/progenitor cells identified by profiling with stem cell markers. PLoS One. 2009; 4:e8377. [PubMed: 20027313]
45. Hennessy BT, Gonzalez-Angulo AM, Stemke-Hale K, Gilcrease MZ, Krishnamurthy S, Lee JS, et al. Characterization of a naturally occurring breast cancer subset enriched in epithelial-to-mesenchymal transition and stem cell characteristics. Cancer Res. 2009; 69:4116–24. [PubMed: 19435916]
46. Balko JM, Jones BR, Coakley VL, Black EP. MEK and EGFR inhibition demonstrate synergistic activity in EGFR-dependent NSCLC. Cancer Biol Ther. 2009; 8:522–30. [PubMed: 19305165]
47. Hollenhorst PC, Shah AA, Hopkins C, Graves BJ. Genome-wide analyses reveal properties of redundant and specific promoter occupancy within the ETS gene family. Genes Dev. 2007; 21:1882–94. [PubMed: 17652178]
48. Marinescu VD, Kohane IS, Riva A. The MAPPER database: a multi-genome catalog of putative transcription factor binding sites. Nucleic Acids Res. 2005; 33:D91–7. [PubMed: 15608292]
49. Barretina J, Caponigro G, Stransky N, Venkatesan K, Margolin AA, Kim S, et al. The Cancer Cell Line Encyclopedia enables predictive modelling of anticancer drug sensitivity. Nature. 2012; 483:603–7. [PubMed: 22460905]
50. Parker JS, Mullins M, Cheang MC, Leung S, Voduc D, Vickery T, et al. Supervised risk predictor of breast cancer based on intrinsic subtypes. J Clin Oncol. 2009; 27:1160–7. [PubMed: 19204204]

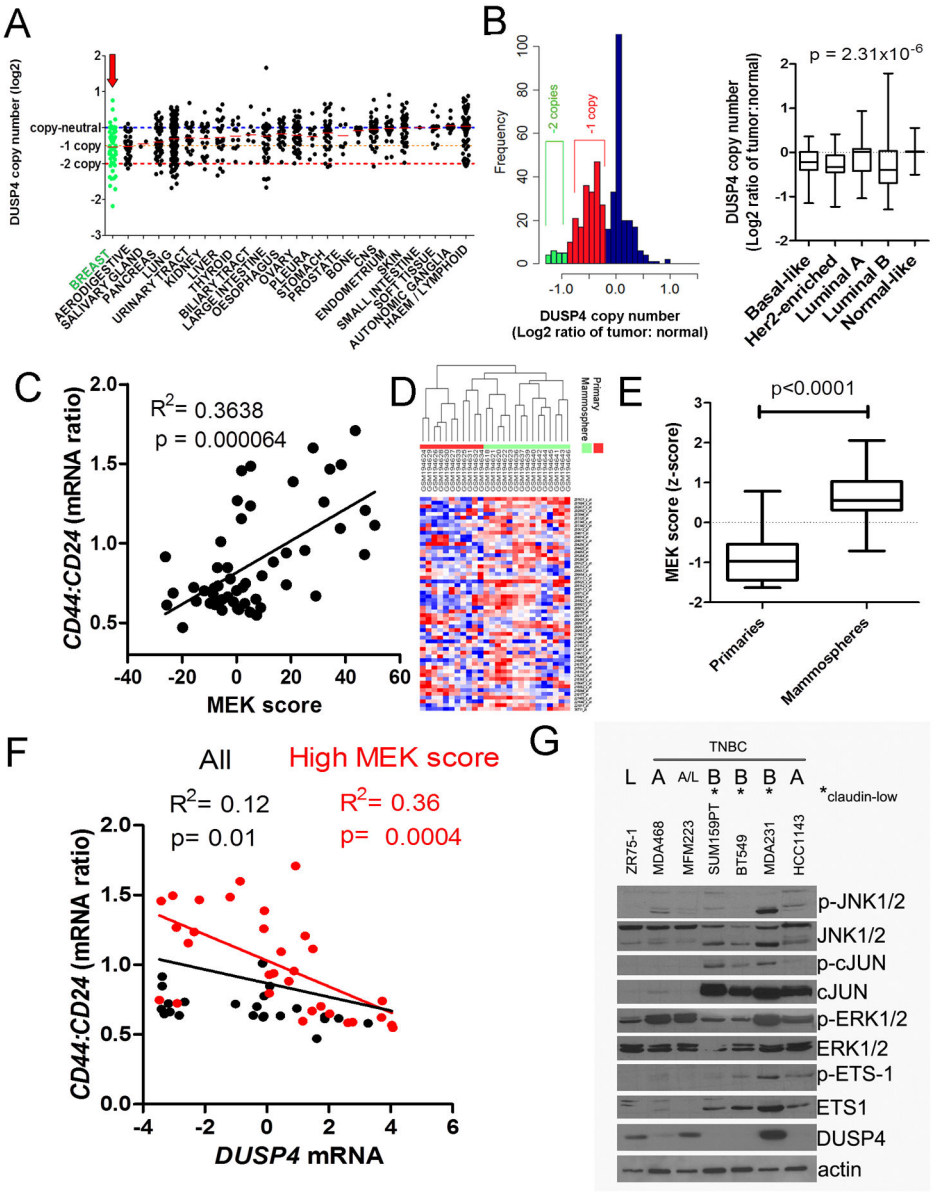

Figure 1. Low DUSP4 and high MEK activation is associated with tumors and cell lines with CSC-like features

A) Cancer Cell Line Encyclopedia data SNP copy number analysis for the DUSP4 locus across 964 cancer cell lines from various tissue sources (49). Red bars show the median log2 copy number for each tissue origin. B) Left panel; frequency histogram of TCGA (14) SNP copy number analysis for the DUSP4 locus for 443 breast cancers normalized to patient matched control tissue (log2 ratio). Right panel; DUSP4 log2 copy number ratio plotted by molecular subtype as determined by gene expression using the PAM50 centroids. P-value represents the ANOVA result. C) CD44:CD24 mRNA ratio for the ICBP50 panel of breast cancer cell lines, as determined by microarray data, plotted vs. the MEK activation score of Pratilas *et al.* (20). D) Unsupervised clustering of RNA from 15 mammosphere cultures vs. 11 primary tumor profiles, representing 16 patients including 10 patient pairs (7) using the genes defined in the MEK signature (20). E) Box and whisker plot of the data in (D),

according to the total sum score of the MEK signature. P-value represents the result of a two-tailed t-test. F) CD44:CD24 mRNA ratio for the ICBP50 panel of breast cancer cell lines, as determined by microarray data plotted vs. DUSP4 mRNA expression. Points and text in black represent the correlation for all cell lines, and points and text in red represent the correlation of only the cell lines with a high MEK activation score (>median of all cell lines). G) Immunoblot analysis of a panel of breast cancer cell lines. TNBC: triple negative breast cancer; L: luminal, A: Basal A; B: Basal B.

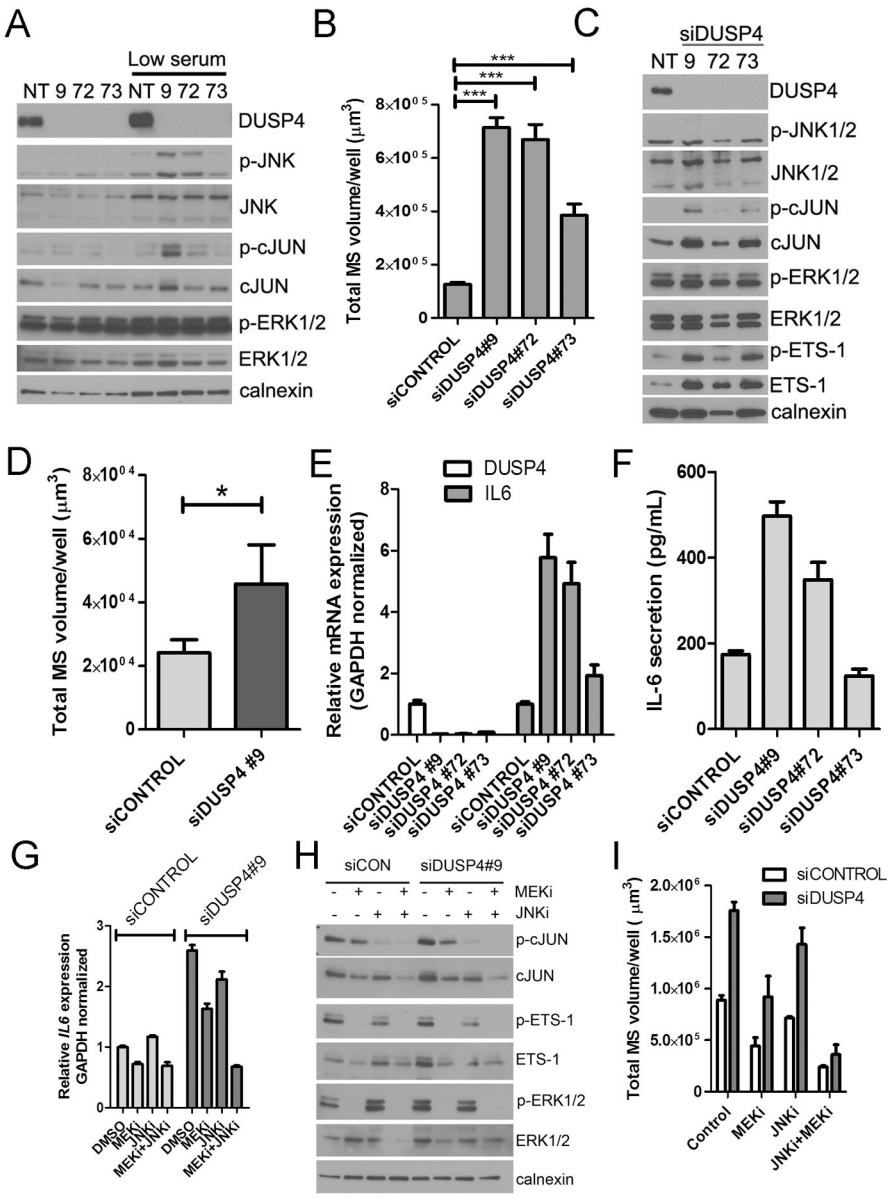

Figure 2. Loss of DUSP4 function upregulates IL-6 and IL-8 and enhances mammosphere growth

A) Immunoblot of MDA-231 cells 96 hrs after siCONTROL or siDUSP4 transfection in 10% FBS containing medium or after 24 hr of serum starvation in 0.1% FBS containing medium B) Mammosphere growth assay in MDA-231 cells, quantitated by GelCount software 6 days after siRNA transfection (5 days after plating to mammosphere culture conditions; ***p<0.001 for a two-tailed t-test). C) Immunoblot analysis performed on lysates from MDA-231 cells grown under non-adherent (mammosphere) conditions. D) Serum-free media was collected 72-96 hrs after siRNA transfection of MDA-231 cells and normalized to cell number. Conditioned medium was added to SUM159PT cells cultured in a mammosphere assay for 5 days and quantitated by GelCount software (*p=<0.05, two-tailed t-test E) qRT-PCR analysis of *DUSP4* and *IL6* mRNA expression in MDA-231 cells 72 hr after siRNA transfection. F) IL6 ELISA in serum-free medium conditioned by siRNA-

transfected MDA-231 cells G) qRT-PCR analysis of *IL6* mRNA expression in MDA-231 cells 96 hr after siRNA transfection and 4 hr after treatment with 1 μM selumetinib (MEKi) or 10 μM SP600125 (JNKi). H) Immunoblot analysis of MDA-231 cells after treatment for 24 hrs with 1 μM selumetinib (MEKi) or 10 μM SP600125 (JNKi). I. MDA-231 mammosphere formation quantitated by GelCount software 7 days after siRNA transfection. Where indicated, selumetinib (MEKi) or SP600125 (JNK1) or the combination was added to the mammosphere cultures. All bars represent the mean of 3 replicates ± SD.

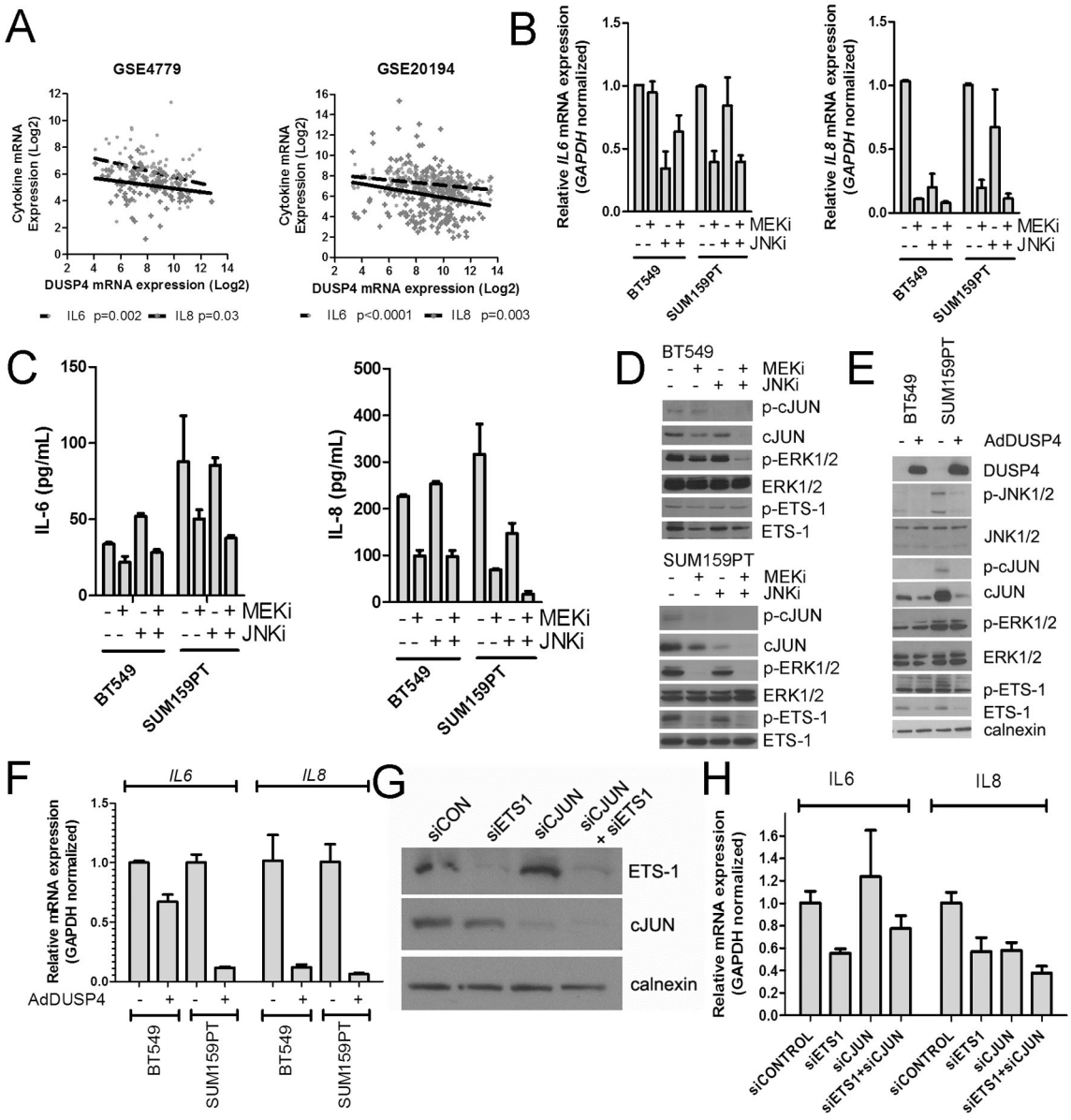

Figure 3. DUSP4 regulates ETS-1 and cJUN and downstream IL-6 and IL-8 expression via MEK and JNK

A) Correlation of *IL6* mRNA and *IL8* mRNA with DUSP4 mRNA in 2 external microarray datasets of primary breast cancer. B) qRT-PCR analysis of BT549 and SUM159PT cells treated for 16 hr with 10 μM SP600125 (JNKi), 1 μM selumetinib (MEKi) or the combination. C) IL6 and IL8 ELISA analyses of conditioned media from BT549 and SUM159PT cells collected after 24-48 hr of treatment with the indicated inhibitors. D) Immunoblot analysis of lysates from cells shown in (B) and (C). E) Immunoblot analysis of BT549 and SUM159PT cells after 16 hr of adenovirus transduction with AdDUSP4 or AdGFP control. F) qRT-PCR analysis of cells from (E). G) Immunoblot analysis of SUM159PT harvested 96 hr after transfection with siCONTROL, siETS-1, siCJUN or the combination. H) qRT-PCR analysis of IL6 and IL8 mRNAs in cells from (G).

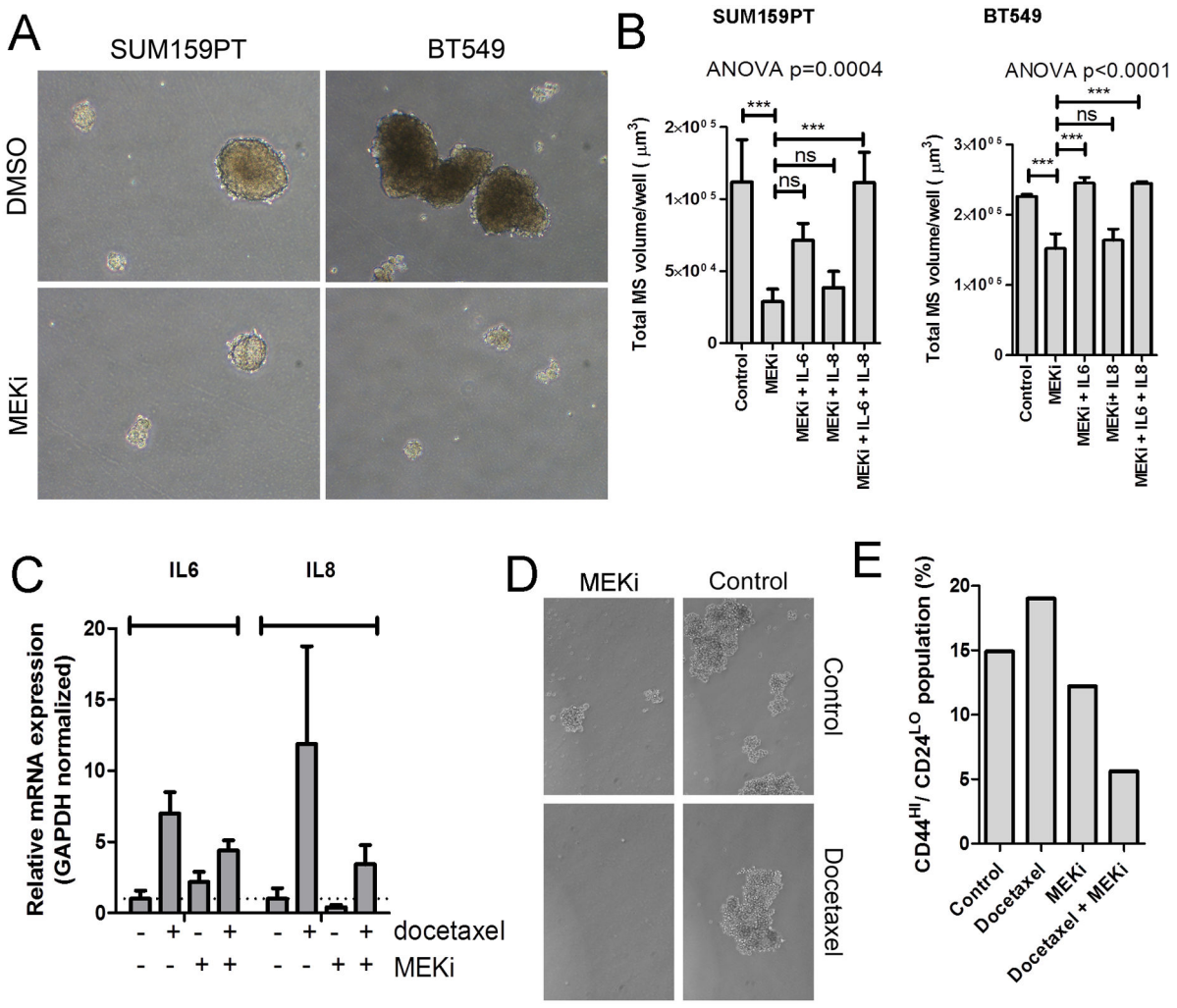

Figure 4. MEK inhibition decreases mammosphere formation in an IL-6/IL-8 dependent manner

A) Representative images of mammospheres derived from SUM159PT and BT549 cells grown in the presence of selumetinib or DMSO. B) Quantification of mammospheres derived from SUM159PT and BT549 cells, grown in the presence of DMSO, selumetinib (MEKi), or selumetinib plus either IL6, IL8, or both IL6 and IL8. P-value represents the result of an ANOVA with Tukey's post hoc test to compare individual treatment groups (***P<0.001). Bars represent mean of 3 replicates ± SD. C) qRT-PCR analysis of IL6 and IL8 mRNAs in MDA-231 xenografts treated for 3 days with docetaxel, selumetinib or the combination (16). D) MDA-231 xenografts treated for 4 weeks with docetaxel, selumetinib or the combination(16) were harvested; cells were mechanically and enzymatically dissociated and plated in a mammosphere assay as described in Methods. E) CD44/CD24 FACS analysis of cells dissociated from MDA-231 xenografts from (D).

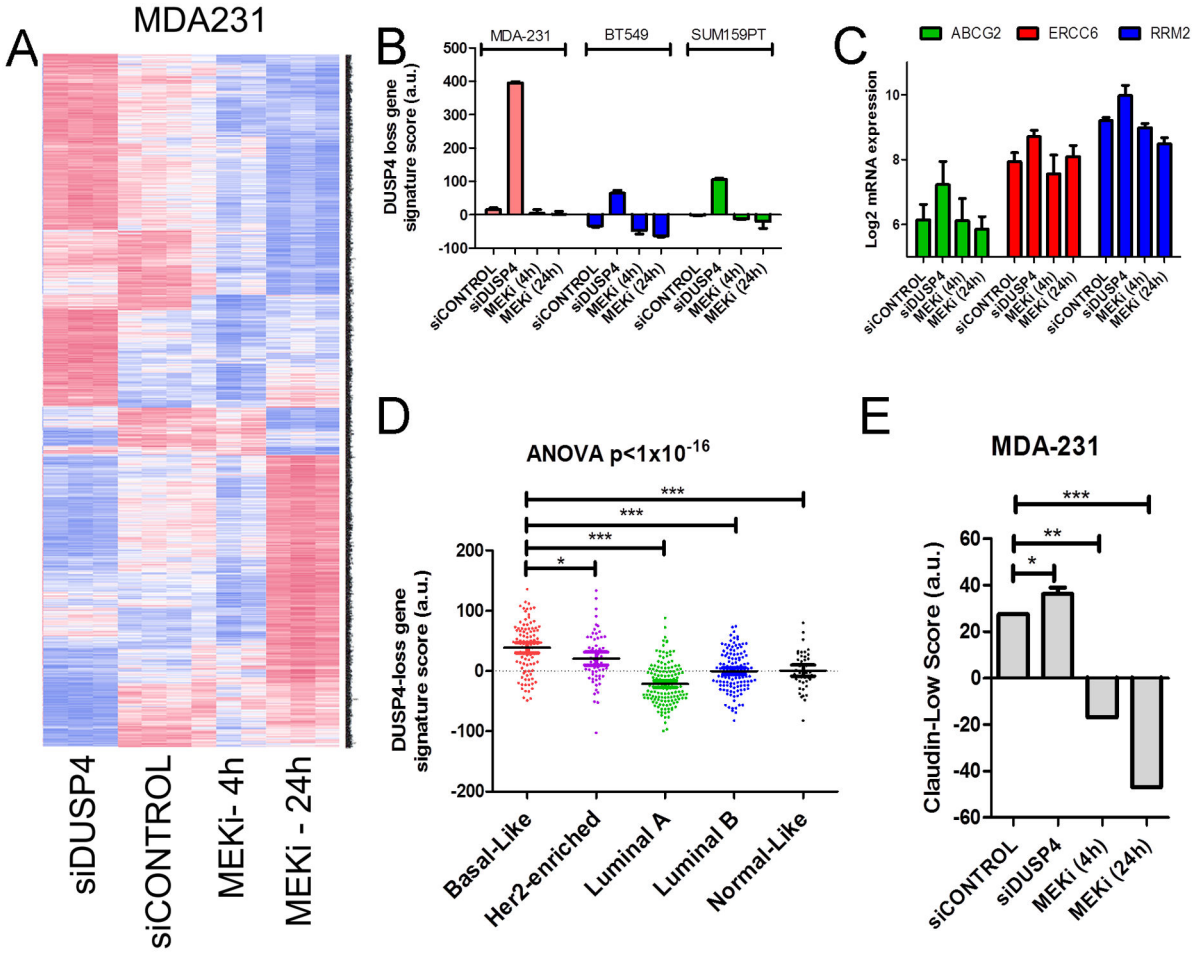

Figure 5. Gene expression patterns of loss of DUSP4 function correlate with basal-like and claudin-low subtypes

Microarray analysis was performed on RNA derived from MDA-231, BT549 and SUM159PT cells 96 hr after transfection with siCONTROL or siDUSP4 and after 4 hr or 24 hr of selumetinib treatment. A) Heatmap of significantly altered genes for MDA-231 cells (ANOVA FDR-adjusted $p<0.01$). B) DUSP4 loss gene expression score derived from MDA-231 cells transfected with siDUSP4 was calculated across all samples. C) Expression of selected chemotherapy-resistance genes which were altered in MDA-231 cells transfected with siDUSP4. D) DUSP4-loss gene expression score derived from MDA-231 cells transfected with siDUSP4 was calculated across 444 tumors in the TCGA breast data. Molecular subtype was determined using the PAM50 centroids (50) and the genefu package in R. E) Association of the claudin-low nine-cell line predictive genes with MDA-231 cells following siDUSP4 or selumetinib treatment (5).

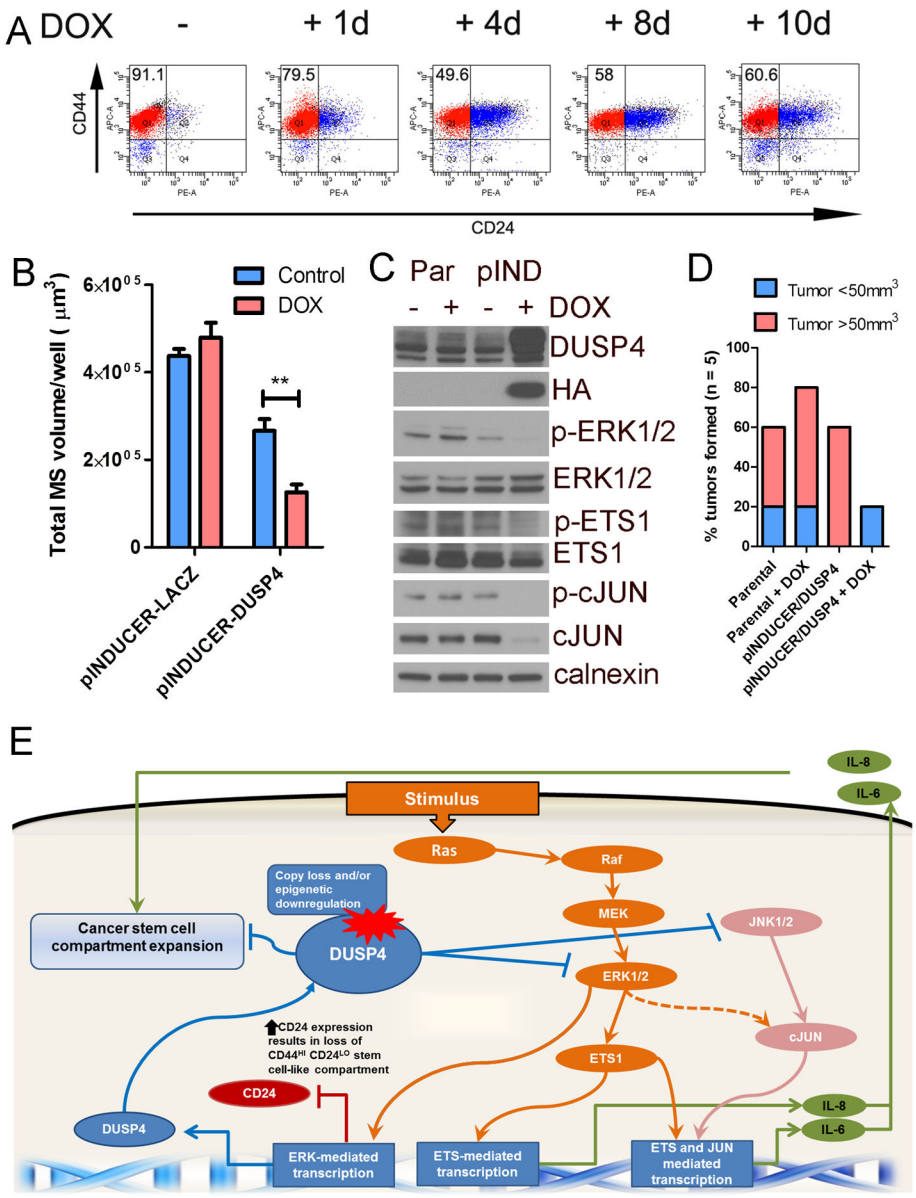

Figure 6. DUSP4 is a tumor suppressor that modulates the CD44^{+}/CD24^{-} stem-enriched population and tumor formation

SUM159PT cells transduced with DOX-inducible DUSP4-HA were generated. A) Flow cytometry analysis of CD44/CD24 expression in cells treated for 1-10 days with DOX (2 ng/mL). B) SUM159PT/pINDUCER-LACZ cells or SUM159PT/pINDUCER-DUSP4 pre-treated for 4 days ± DOX prior to plating in a mammosphere assay in the presence or absence of DOX as in the pretreatment. C) Immunoblot of parental SUM159PT/pINDUCER-LACZ cells or SUM159PT/pINDUCER-DUSP4 treated for 4 days with DOX. D) Tumor formation of cells from (C) 60 days after injection the mammary fatpad of athymic mice. Red bars indicate palpable tumors and blue bars indicate tumors identified on histological examination of the injection site. E) Schematic of proposed model based on the presented data: The tumor suppressor DUSP4 negatively regulates ERK and JNK. Upon loss of DUSP4, derepressed ERK and JNK activity stimulates ETS1 and cJUN-mediated

transcription of IL6 and IL8, cytokines that expand the cancer stem-like cell population. De-repressed ERK transcription following DUSP4 loss also suppresses CD24 expression thus increasing the $CD44^{HI}$ $CD24^{LO}$ compartment, a marker of the CSC population.